

The Charge Transport in Organic Field-Effect Transistor as an Interface Charge Propagation: The Maxwell–Wagner Effect Model and Transmission Line Approximation

Martin Weis*, Jack Lin, Dai Taguchi, Takaaki Manaka, and Mitsumasa Iwamoto†

Department of Physical Electronics, Tokyo Institute of Technology, 2-12-1 O-okayama, Meguro, Tokyo 152-8552, Japan

Received February 27, 2010; revised March 28, 2010; accepted April 13, 2010; published online July 20, 2010

By analyzing electric field migration in the pentacene organic field-effect transistor channel (OFET), visualized using the time-resolved microscopic optical second harmonic generation (TRM-SHG) is analyzed the propagation of injected carriers. We find that the accumulated charge propagation on the pentacene–gate insulator interface of the three-electrode system is clearly different from the drift in electric field of the two-electrode system. The propagation of injected carriers is evaluated on the basis of the Maxwell–Wagner effect model and the transmission line approximation. We show that the interface charge accumulation has a significant contribution to the charge transport in OFET. Proposed model for the transient state is beyond the limits of common used impedance spectroscopy models and represents extension of the small-signal analysis. Found relation between mobility and transit time helps in analysis of OFET transit time sensitive experiments such as the time-of-flight technique (TOF) or TRM-SHG. © 2010 The Japan Society of Applied Physics

DOI: 10.1143/JJAP.49.071603

1. Introduction

Semiconductor devices using organic materials,^{1,2)} such as thin film transistors^{3–5)} and light emitting diodes⁶⁾ have attracted a lot of research interests. With the development of organic materials with high mobilities, recent research focus on the organic field-effect transistor (OFET) has been concentrated on the applied research mostly to increase the carrier mobility. Towards this many experimental approaches have been exerted such as modification of the surface gate insulator, use of single crystal semiconductor layer, etc.^{7–9)} In addition to the experimental techniques, the importance of the basic research such as injection, accumulation and transfer mechanisms is being recognized to improve the OFET performance. However, owing to the ambiguities of energetic at the organic–metal and organic–organic interfaces, device performance is not fully understood. That is, the device physics of OFET is not yet clear in comparison with that of inorganic FET structures. Beyond that transient phenomenon of carrier propagation is without deep understanding.

Carrier transport through the OFET as a transient phenomenon has not been investigated for a very long time.^{10,11)} Difficulty had an origin mostly in experimental problems as well as deep study of the steady-state only. However, recently there was a research focused on the time-of-flight (TOF) method applied on the OFET structures^{11,12)} and transit time t_{tr} was obtained. Subsequently, the analysis of the carrier mobility μ was carried out in accordance to the following relation

$$t_{tr} = \frac{1}{\mu} \frac{L^2}{V_{ds}}, \quad (1)$$

where L was the channel length and V_{ds} was drain–source voltage. Although this approach is very intuitive and based on the experience with two-electrode structures, there is no deep argument to use drain–source voltage in OFET structure for mobility evaluation. It is assumed only that carrier transport is described as the drift in the average electric field V_{ds}/L at a constant velocity $v = \mu V_{ds}/L$. Later

TOF study of Dost *et al.*¹³⁾ suggested using the drain–source voltage reduced by the threshold ($V_{ds} - V_{th}$) instead of V_{ds} . This result was supported by the experiment, even though the detail explanation was not clear. On the other hand, various studies have already reported the square root of time law^{14–16)} by the small signal analysis which represents measurement without distortion of the steady-state. Hence, question on the transient state caused by the larger disturbance is still unanswered.

Additionally, understanding to the carrier transport as a transient phenomenon is crucial also for other transient measurements like a time-resolved microscopic second harmonic generation (TRM-SHG).^{17,18)} Of course, understanding of transient behaviour is crucial from view points of device application such as switching and high speed elements. TOF measurement is an elegant way, but it is an indirect method and it merely probes displacement current caused by the change of induced charges on electrodes. Hence, TOF gives a transit time crossing the channel, but cannot give a physical picture of carrier motion without an elaboration of the mathematical analysis. On the other hand, the TRM-SHG technique that we are developing is able directly to visualize the SHG intensity propagation in the channel region of the OFETs by a two-photon process. Because the SHG intensity is proportional to the square of electric field and subsequently is determined by the carrier distribution, TRM-SHG technique possesses great potential in exploring carrier dynamics in the OFETs. Using the TRM-SHG measurement, carrier injection and transport processes are individually examined. This property gives us a strong tool to study charge propagation only, without influence of the injection behaviour. Additionally, by the TRM-SHG measurement it was already shown that the electric field of the carrier sheet is migrating through the channel with the square root of time.¹⁷⁾ The meaning of experimental finding of the square root time dependence of charge propagation is quite important, though it has been predicted by using some physical models.¹⁹⁾ Because we can truly check the validity of physical models proposed. That is the mechanism of the carrier transport is not fully understood regardless of the direct visualizing of the field propagation. Therefore, these experiments call our attention and carrier transport mechanism needs to be explained.

*On leave from Institute of Physics, Slovak Academy of Sciences.

†E-mail address: iwamoto@ome.pe.titech.ac.jp

2. Model

Two physical models of charge carrier transport are presented and discussed, the Maxwell–Wagner (MW) model and the transmission line approximation. The MW model is well-known for physical explanation of charge accumulation on the interface,^{20,21} and relies on the microscopic electrical properties of materials. On the other hand, the transmission line approximation is common for signal propagation analysis, and relies on equivalent circuits. Both models are used to explain the charge propagation in two- and three-electrodes systems represented by metal–insulator–metal (MIM) and OFET structures. We show that both models approach to the same result. In other words, the transmission line approximation can model the charge propagation across the channel even though conductivity distribution changes with time. Comparison of models points out advantages as well as limits of both evaluations.

2.1 The Maxwell–Wagner model

Two macroscopic physical parameters characterize organic materials used in MIM and OFET. These are dielectric constant ϵ and conductivity σ , respectively. The ratio ϵ/σ gives a relaxation time and stands for spreading time of excess charge carriers in the materials. That is a steady-state charge distribution is established after an elapsed time around $\tau = \epsilon/\sigma$. Note that conductivity is in proportion to carrier density n_0 , and give by $\sigma = en_0\mu$. The carrier density n_0 is generally intrinsic carrier density of materials at thermodynamic equilibrium. According to the electro-magnetic field theory, total current flowing across organic materials is sum of the conduction current and the displacement current. The current density j of conduction current and displacement current is given by σE and $\partial D/\partial t$ with $D = \epsilon E$, respectively. Here E is electric field and D is electric flux density. For the MIM structures, when injected carrier density n is low but it continuously supplied from electrodes, and space charge field caused by injected carriers is negligible in comparing with applied external electric field (linear potential through the insulator part), σE and ϵE are replaced by $\sigma V/L$ and $\epsilon V/L$, respectively. L is the thickness of the insulator. This means that the MIM structure is represented merely as a parallel electrode system $R = L/\sigma S$ and $C = \epsilon S/L$ in the light of carrier transport of injected carriers. Obviously, we find the relationship between the time constant of the equivalent circuit RC and the relaxation time of the insulator ϵ/σ as $RC = \epsilon/\sigma$. That is the time constant RC is free from geometry of electrode configuration, and it is given only by material parameters, σ and ϵ . From the equivalent circuit consideration, we find the equivalent circuit is converted into N -series parallel RC circuit, as illustrated in Fig. 1(a), suggesting potential drop of each resistance R/N and charging of each capacitance NC must be the same: no charge accumulation at the connection point between segments. According to the MW effect, charge accumulation happens at the interface between two materials with different relaxation times. Hence, in an insulator represented by constant material parameters ϵ and σ , there is no charge accumulation like trapped carriers over the whole region, and merely carriers are supplied from one electrode and they are conveyed to the counter electrode

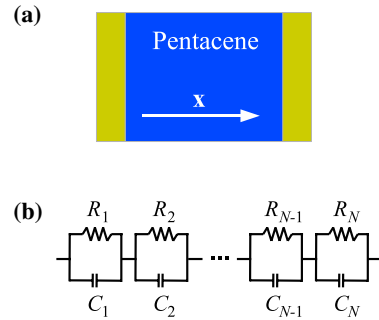


Fig. 1. (Color online) (a) Sketch of a pentacene MIM structure and (b) its equivalent circuit with distributed parameters.

across the insulator. This is actually consistent with the result of the N -series RC circuit model, illustrated in Fig. 1(a). The transit time of carriers across the MIM structure is given by

$$t_{tr} = \frac{L}{\mu E} = \frac{L^2}{\mu V}, \quad (2)$$

and a steady-state current flows at $t = t_{tr}$ after applying a step voltage V at $t = 0$.²² Obviously, we may consider this time t_{tr} gives a charge spreading time $\epsilon/\sigma = \epsilon/en\mu$, where n is the sum of the average carrier density of the insulator caused by injected carriers and intrinsic carriers, n_0 . Therefore we obtain the relation $en = (\epsilon V/L)/L$, representing a constant carrier distribution in the MIM after the time t_{tr} . In other words, the carrier density of the dielectric changes from n_0 to n at $t = t_{tr}$. This discussion can easily extend to the case where carriers transit across i -series RC segments ($i < N$), i.e., from electrode to i -connection point in the equivalent circuit shown in Fig. 1(a).

In that situation, the time required carriers crossing the i -segments is given by

$$t'_{tr} = \frac{L'}{\mu E} = \frac{L'^2}{\mu V'} \quad (3)$$

with

$$L' = \frac{i}{N}L \quad \text{and} \quad V' = \frac{i}{N}V.$$

As the charge spreading into the i -segments from the electrode should be the same as $\epsilon/\sigma = \epsilon/en\mu$ we obtain $en = (\epsilon V'/L')/L'$. That is, the carrier density of the insulator changes from n_0 to n , along with the evolution of the region of injected carriers in the presence of electric field E . Therefore we may conclude that charge transport in two-electrode system can be simply described by the drift of carriers in the average electric field, on satisfying the square root of time dependence along the direction of the electric field.

The situation is quite different in the case of OFET. As we described above, at the interface between two materials with different relaxation times, charge is accumulated at the interface. This situation happens at the active organic layer–gate insulator interface. The relaxation time of gate insulator material is longer than that of active layer, $\tau_{ins} > \tau_{act}$. Therefore, charge is accumulated at the interface in a manner like trapped charges while a current flows, and this

situation is quite different from that of MIM, and suggesting that carrier motion must be described using a model with consideration of interface charge accumulation.

In more detail, for the OFETs, carriers are injected from the source electrode in a manner similar to the case of the MIM structures, but they flow along the gate insulator–active layer interface in the direction from the source to the drain electrode, accompanying interface charge accumulation caused by the MW effect. In detail, interface charge Q_s is induced by the difference in electric displacement fields, $Q_s = \nabla \cdot D = \nabla \cdot (\epsilon/\sigma)j$. Here j is the current density flowing across the interface. This relation results to product of capacitance and voltage regulated by the difference of the layers relaxation times, $Q_s = CV(1 - \tau_1/\tau_2)$, where C is the capacitance with higher resistivity, and V is the voltage applied to the capacitance. For pentacene film and SiO₂ are reported conductivities of 2×10^{-5} S/m²³) and 10^{-18} S/m. Thus, for comparable dielectric constants of pentacene and SiO₂ of 4 and 3.8 we receive relaxation time τ of pentacene significantly shorter than in the case of SiO₂. Hence, the amount of charge accumulated at the interface is regulated by applied voltage only, and it is approximately given by

$$Q_s = C_g \left(V_{gs} - V_{th} - \frac{1}{2} V_{ds} \right), \quad (4)$$

where in the limit linear potential is built along the interface by spreading of accumulated charge along the organic semiconductor–gate insulator interface. Although eq. (4) is similar to the conventional model used in semiconductor physics, the background theory is different as written above. Here, C_g and V_{gs} are gate insulator capacitance per unit of area and gate–source voltage, respectively. V_{th} is threshold voltage, generally caused by trapped carriers, interfacial states, etc. The carrier density at the active layer–gate insulator interface changes from n_0 to n caused by Q_s . Therefore, in a similar consideration to the case of the MIM structure, we may can estimate a spreading time of the charge carrier at the interface. As the carrier density is given by $en = C_g(V_{gs} - V_{th} - V_{ds}/2)/h$ (h : channel thickness), the conductance along the interface is given by

$$G = \frac{en\mu Wh}{L}. \quad (5)$$

On the other hand, charge accumulation is regulated by the potential across gate insulator as described by eq. (4), the capacitance along the channel is given by

$$C = C_g LW. \quad (6)$$

Hence, the response time is given as C/G , and represents a carrier transit time t_{tr} across the interface from the source to drain. That is,

$$t_{tr} = \frac{L^2}{\mu \left(V_{gs} - V_{th} - \frac{1}{2} V_{ds} \right)}. \quad (7)$$

We should note that the transit time t_{tr} is also valid for the case $V_{ds} = 0$, and represents charge accumulation condition at the interface only. Hence, it is reasonable to talk that interface charge propagation process regulates the transit time of OFETs. Further we should note that in the derivation of eq. (4), we assumed $|V_{gs} - V_{th}| \gg |V_{ds}|/2$ as the most

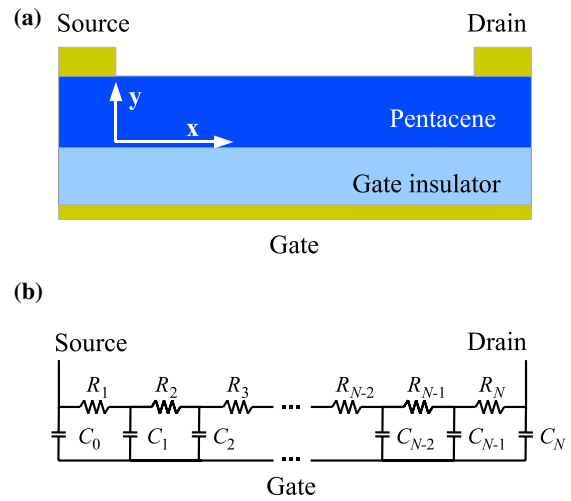


Fig. 2. (Color online) (a) Sketch of a pentacene OFET and (b) its equivalent circuit in transmission line approximation.

simple case, but the above discussion can extend to other cases without loss of behind physics.²⁴⁾ In addition, although above analysis is based on common used steady state potential distribution across the channel, it can be extended to time-dependent accumulation of the interface charge.

It is instructive to note that this situation can be modeled using an equivalent circuit shown in Fig. 2(b), where the resistance corresponds to the conductance G along the channel, and the capacitance represents the capacitance C of eq. (6). In Fig. 2(b), the potential distribution along the channel is considered, and the equivalent circuit is extended to a ladder model. The transmission line model is based on this equivalent circuit, as will be discussed in §2.2. Further we should note that in derivation of eq. (7) we assumed carrier injection to the interface is only from the source electrode, but t_{tr} should be reduced in case carrier injection is also allowed from the drain. For instance, t_{tr} should be half of the t_{tr} of eq. (7) when $V_{ds} = 0$ instead of $V_{ds} = V_{gs} - V_{th}$ and we use similar electrodes as the source and drain electrodes.

2.2 The transmission line approximation

The TOF method was originally designed for the metal–semiconductor–metal (MIM) structures,^{25–28)} where carrier transport in the system of two electrodes is possible to be described as an one-dimensional problem [see Fig. 1(a)]. Interestingly, the propagation of charges can be solved also by the equivalent circuit with distributed parameters [Fig. 1(b)]. The equivalent circuit stems from Maxwell’s basic idea that a current flowing inside a material is given as the sum of conduction current and displacement current. R and C represent these two contributions, respectively. On the other hand, these elements of the equivalent circuit stand for the physical phenomenon: a network of R ’s and C ’s illustrates the distributions of electric field and charge. In detail, the constant electric field (i.e., linear potential through the semiconductor part of the MIM structure) is modelled by equal resistor R representing a potential drop per distance dx . In this model, the charge is propagating from one electrode with area S to the opposite one situated in distance d through the resistors and the charge carrier distribution is depicted

by the capacitors C . Here it is assumed no electric field inside a metal electrode ($C_{\text{metal}} = 0$) and negligible metal resistance compared to semiconductor ($R_{\text{metal}} = 0$). Hence, if e and n are the elementary charge and carrier density, respectively, the distributed conductance σ can be estimated from the current density as follows:

$$J = en\mu E = \frac{CV}{d} \mu \frac{V}{d}, \quad (8)$$

by the differentiation of the current density with respect to E , defined as $\sigma = \partial J / \partial E$. Subsequently, distributed resistance $R = d / (\sigma V)$ is extracted:

$$R = \frac{d^2}{CS\mu V}. \quad (9)$$

Although excess mobile charges are injected into the device, in this evaluation it is assumed that the effect of a space-charge field is negligible. That is the reason we derive the σ using $en\mu E$, not the last term of eq. (8). Thus the electric field across the MIM structure is constant, $E = V/d$. If a voltage pulse with an amplitude V is applied to the electrodes, the transit time, which is represented by the relaxation time of the semiconductor of the MIM structure, can be simply estimated by the relation $t_{\text{tr}} = RC$ and therefore

$$t_{\text{tr}} = \frac{1}{\mu} \frac{d^2}{V}. \quad (10)$$

Note that here the product of RC has a meaning of the relaxation of the injected carriers, and $t_{\text{tr}} = RC$ with $R = \sum R_i$ and $C = \sum C_i$ (and $R_i = R_j$, $C_i = C_j$ for all i, j) represents the carrier transport time across all RC segments illustrated in Fig. 1(b). In limit of infinitesimal small elements the sum is replaced by the integration $t_{\text{tr}} = (1/L) \int_0^L RC dL = RC$ with identical result. As such the transit time t_{tr} of eq. (10) expresses the situation where charge carriers are conveyed through a series of RC segments in the whole MIM structure. This is described by the transit time dependence on the voltage V and the film thickness d . Since there is no difference between the relaxation times of RC loops, no excess charge is stored between the series RC segments. This means that all charge carriers get transported across the MIM structure, even though they contribute to the space charge field formation. Presented model with distributed parameters describes this situation, and accounts for no charge accumulation corresponding to charge trapping in the insulator layer in the MIM structure.²⁴⁾ Therefore charge transport can be simply described by the drift of carriers in the average electric field. Furthermore, eq. (10) suggests that carriers will propagate with the square root of time in a drift field along the direction of the electric field intensity. In summary, we may conclude that the transit time t_{tr} is dependent on the geometrical parameter as well as applied voltage. In the following text, we discuss a case of the OFET structures and derive the transit time t_{tr} given by eq. (14).

It is instructive to note that in the state of the thermodynamic equilibrium the dielectric relaxation time, defined by RC , is a material parameter defined by ϵ / σ , where ϵ and σ are the dielectric constant and conductivity, respectively. The dielectric relaxation time becomes independent of the

geometrical parameter as well as applied voltage. Here σ is proportional to the product of carrier density in equilibrium state n and mobility μ . Hence, the value of RC for MIM structures and OFETs should be the same. Note that above description is only valid when we consider the carrier transport across the bulk where the excess carrier contribution is dominant. eq. (10) becomes invalid when we describe the carrier transport along the semiconductor–insulator interface.

The electric field propagation along the channel in an OFET [Fig. 2(a)] was recently successfully modelled by the transmission line approximation (TLA).²⁹⁾ TLA is based on solving the equivalent circuit consisting of infinitesimally small resistors and capacitors connected in series as a ladder [Fig. 2(b)]. In this model, charges are propagating through the channel at the pentacene–gate insulator interface. Therefore again, the resistor R and capacitor C are related to the distributions of the electric field and accumulated charge [$q_s(x) = C \partial V(x) / \partial x$]. In other words, the successive charging of the capacitors C represents the migration of charge carriers and resistances R describe the potential drop V across the channel. Note that in the presented model of the three-electrode system (OFET structure) we do not assume the influence of injection properties, i.e., potential drop due to an injection barrier, which causes insufficient charge accumulation. Also the displacement current between source and drain electrodes is assumed negligible by taking into account the electrode size and separation used in this experiment. In summary, with consideration of the device parameters, the parallel segmental capacitance, found in the equivalent circuit for the MIM structure and employed to express carrier transport as displacement current, is discarded in the equivalent circuit for the OFET channel [see Fig. 2(b)]. Furthermore, as the conductivity of the gate insulator of our OFET device is extremely low, the parallel resistance element to express the carrier transport across the gate insulator is omitted in the equivalent circuit.

In the following, analogous to the analysis of the MIM structure, the charge transport can be again solved by the relaxation times of RC loops with distributed parameters. In the linear region (drain–source voltage is smaller than gate–source voltage, $|V_{\text{ds}}| \ll |V_{\text{gs}} - V_{\text{th}}|$) the constant electric field condition should be satisfied and all resistors of the equivalent circuit have identical values. Therefore, the transit time can be written as a product of the channel resistance R_{ch} and capacitance C_{ch} , i.e., $t_{\text{tr}} = R_{\text{ch}} C_{\text{ch}}$. The drain–source current I_{ds} can be expressed³⁰⁾ as

$$I_{\text{ds}} = C_g \frac{W}{L} \mu \left(V_{\text{gs}} - V_{\text{th}} - \frac{1}{2} V_{\text{ds}} \right) V_{\text{ds}}, \quad (11)$$

where C_g is the gate insulator capacitance per unit of area, W/L is the channel width/length and $V_{\text{gs}} - V_{\text{th}}$ is the applied gate–source voltage, V_{gs} , reduced by the threshold voltage, V_{th} . However, in contrast to the small signal analysis here we apply large signal which propagates across the channel. In other words, charges carry the electric field and therefore the voltage drop varies with charge carrier (i.e., potential) distribution. Therefore, the channel resistance is not constant anymore and depends on time and position $R_{\text{ch}} = R_{\text{ch}}(x, t)$. For a linear approximation of the potential distribution

between the source electrode edge ($x = 0$) and the charge carrier sheet edge in the channel region ($x = x^*$) is derived as

$$R_{\text{ch}}(x) = \frac{V_{\text{ds}}}{I_{\text{ds}}} = \frac{x^*}{C_{\text{g}} W \mu \left(V_{\text{gs}} - V_{\text{th}} - \frac{1}{2} V_{\text{ds}} \right)}. \quad (12)$$

The channel capacitance follows:

$$C_{\text{ch}} = C_{\text{g}} W L, \quad (13)$$

where $W L$ represents the channel area. Therefore, the transit time can be written as a product of eqs. (12) and (13) in the form

$$t_{\text{tr}} = \frac{1}{L} \int_0^L R_{\text{ch}} C_{\text{ch}} dx^* = \frac{1}{2\mu} \frac{L^2}{V_{\text{gs}} - V_{\text{th}} - \frac{1}{2} V_{\text{ds}}}. \quad (14)$$

It is interesting to note that identical result from definition of the group velocity can be also obtained:

$$v_{\text{g}} = \frac{dx}{dt} = \mu E. \quad (15)$$

Here, we assume linear potential profile, $E = V'/x$ (for $x \leq x^*$) or $E = 0$ (for $x > x^*$), with effective voltage V' . Trivial integration of eq. (15) for $x \in (0, L)$ and $t \in (0, t_{\text{tr}})$ provide us simple relation

$$t_{\text{tr}} = \frac{1}{2\mu} \frac{L^2}{V'}. \quad (16)$$

Note that the MW model and TLA gives identical result for the MIM structure [see eqs. (2) and (10)]. On the other hand, the transit time estimated by MW model [eq. (7)] and TLA [eq. (14)] differs by factor 1/2 only. This deviation has an origin in time dependent conductivity, which reflects changes of electric field during the charge propagation. In addition, this confirms also the trivial analysis of the transit time, eq. (16).

As mentioned above we could reach the same conclusion starting from the MW model and TLA model. One of the important findings from these two approaches is that the transit time t_{tr} , defined by eqs. (7) and (14), is valid even when $V_{\text{ds}} = 0$. This represents that interface charge propagation regulates transient carrier transport in the OFET channel. In the following sections, we evidently show such situation by using TRM-SHG measurements.

3. Experiment and Results

Samples used in the experiments were top-contact pentacene OFETs. Heavily-doped Si wafers with a 500-nm-thick thermally prepared silicon dioxide (SiO_2) insulating layer were used as the base substrates. A 100-nm-thick poly-(methyl methacrylate) (PMMA) layer was spin-coated onto the Si wafers prior to the deposition of pentacene (100 nm in thickness) in order to improve on-off ratio of the devices. The spin-coated film was deposited from chloroform solution using the following two steps: (1) at 2130 rpm for 5 s and (2) at 2500 rpm for 30 s. The gate insulator capacitance C_{g} was 5.37 nF/cm². During the deposition of pentacene, the pressure was kept at less than 10^{-4} Pa and the deposition rate was fixed at 0.5 Å/s, monitored by using a quartz crystal microbalance. After the deposition of pentacene,

gold electrodes (source and drain electrodes) of a thickness of 50 nm were deposited on the pentacene surface. The designed channel length (L) and width (W) were 45 μm and 3 mm, respectively. The measurement of the transient states was performed with: (i) positive potential applied to the source electrode with grounded drain and Gate electrodes, in this setup: $V_{\text{gs}} = V_{\text{ds}} = -100$ V, i.e., the OFET switches ON into saturation, or (ii) positive potential applied to both source and drain electrodes with grounded gate electrode, in this setup: $V_{\text{gs}} = -100$ V, $V_{\text{ds}} = 0$ V, i.e., the OFET remains switched ON but drain current ceases. Note that the device was always analyzed in the saturation regime. From a device fabrication perspective, source and drain electrodes are identical. All measurements were performed in laboratory ambient atmosphere.

Selecting an appropriate wavelength is important to observe the SHG signal from pentacene effectively, because the SHG intensity is material dependent and strongly depends on the fundamental wavelength used. According to the electric field induced SHG (EFISHG) spectrum of vacuum deposited pentacene films,³¹⁾ the fundamental wavelength was fixed at 1120 nm in this study. The light source for the SHG measurement was a Nd:YAG laser-equipped with optical parametric oscillator (OPO; Continuum Surelite OPO). The fundamental light was focused onto the channel region of the OFET with normal incidence using a long working distance objective lens (Mitutoyo: M Plan Apo SL20×, numerical aperture: 0.28, working distance: 30.5 mm). The spot size was approximately 150 μm, and the fundamental light almost uniformly irradiated across the channel. Finally, the SH light was detected by a charge-coupled device (CCD) camera (Andor Technology BV420-DR).

4. Discussion

Figure 3 shows a typical TRM-SHG imaging at various delay times under $V_{\text{gs}} = V_{\text{ds}} = -100$ V. With an increasing delay time, the SHG peak moves from the source to the drain electrode and represents the edge of the carrier sheet.¹⁷⁾ Here should be noted that the peak position of the SHG intensity vs the measured time on a \log_{10} - \log_{10} scale reveals a square-root of time dependence (linear fit with slope of 0.47), inset of Fig. 3 illustrates delay time as a function of the square of peak position.

Note that the carriers are predicted to migrate through the device with the square root of time ($x \propto \sqrt{t}$). This result is in accordance with the TRM-SHG experiment shown in Fig. 3 (see inset). However, our calculation has also other important consequences: (i) the charge is propagating through the OFET channel not only due to an electric field between source and drain electrodes, but also due to an interface charging phenomenon; (ii) the charge is redistributing and accumulating within the channel also when no drain-source voltage is applied. In detail, in the three-electrode system we found a different mechanism for the carrier transport. In contrast to the two-electrode system represented by the MIM structure, where the transport mechanism is limited by charge carrier drift in the electric field, in the three-electrode system (OFET structure) the charge is transported due to the propagation of interface charges (i.e., propagation of the accumulated charge layer).

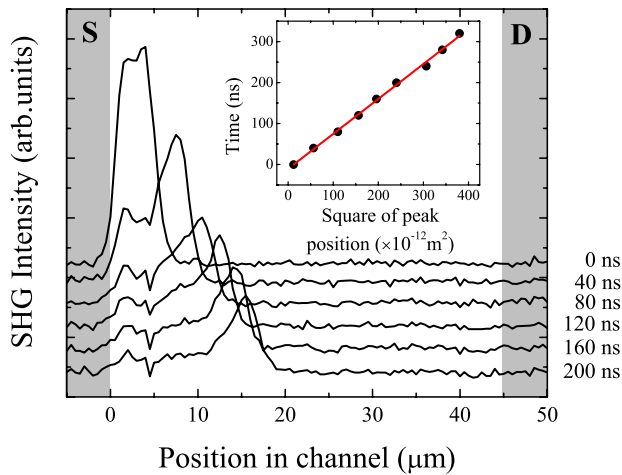


Fig. 3. (Color online) The SHG profiles for a pentacene OFET depicted for various delay times after application of a positive voltage pulse to the source electrode ($V_{ds} = V_{gs} = -100$ V). Gray colored regions indicate the electrodes. Inset illustrates delay time dependence on the square of the peak position. Solid line represents linear fit.

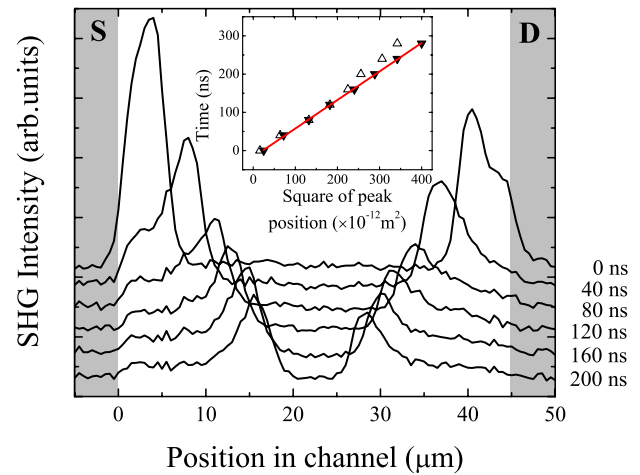


Fig. 4. (Color online) The SHG profiles for a pentacene OFET with electrically shorted source and drain electrodes depicted for various delay times after application of a voltage pulse ($V_{ds} = 0$ and $V_{gs} = -100$ V). Gray colored regions indicate the electrodes. Inset illustrates delay time dependence on the square of the peak position, where up and down triangle represent propagation from source and drain electrodes, respectively. Solid line represents linear fit.

In other words, in the MIM structure with a single layer of dielectric material (pentacene) carriers are transported directly in the direction of the electric field. On the other hand, in the OFET structure comprising a two-layer system (pentacene and gate insulator) charge transport is due to the charging of semiconductor–gate insulator interface and carrier motion is near perpendicular to the external gate field.¹⁷⁾ Note that the motive force, which conveys carriers within the channel, is due to the local electric field generated by injected excess charges. The lateral component of local electric of the excess charges cause a redistribution and migration within the channel toward the steady state condition. Additionally, interface charging, which is very similar to the carrier trapping, but originally caused by the MW effect between the pentacene and gate insulator layer,²⁴⁾ is a characteristic phenomenon originating in an OFET system. Although the carrier migration through both configurations (i.e., $V_{ds} = -100$ or $= 0$ V) follows a square root of time law the physical reason is different. In detail, the charge should be transported by the carrier drift (i.e., field between the source and drain electrodes, which is proportional to V_{ds}) or by the interface charging (i.e., field between the source and Gate electrodes, which is proportional to V_{gs}). This conclusion is in accordance with the SHG experiment, where the OFET had been electrically connected according to configuration (ii) and the electric field of the injected carriers also migrates when the source and drain electrodes have the same potential (are electrically shorted) (Fig. 4). The TRM-SHG recordings also show the charge migration to start out symmetrically from either electrode towards the channel center (22.5 μm) due to the absence of a directional drift force between source and drain. As is illustrated by the inset of Fig. 4 carriers migrate from both source and drain electrodes identically and follow propagation depicted in inset of Fig. 4. Moreover, analysis of the carrier sheet migration again shows a square root of time dependency. Here we must point out that, although no drift field between source and drain electrode is established, observed carrier propagation is not related to the diffusion process, which is

significantly slower in organic semiconductors. This result is in accordance with previous work of Bürgi *et al.*¹⁹⁾ Intriguingly, this experimental study is in agreement with proposed carrier transport based on the phenomenon of the interface charging [see eq. (14)], whereas the carrier drift approach contradicts this result. Experimental methods sensitive to the transit time of the OFET device are the TRM-SHG and the TOF. Equation (14) provides a way for estimating carrier mobility by both methods.^{12,32)} In detail, the OFET mobility for device illustrated in Fig. 3 reaches value of $0.094 \text{ cm}^2 \text{ V}^{-1} \text{ s}^{-1}$ and the TRM-SHG mobility estimated by eq. (14) has a value of $0.099 \text{ cm}^2 \text{ V}^{-1} \text{ s}^{-1}$. It was also shown that using this evaluation method experimental techniques like TRM-SHG and TOF give a mobility comparable with that one obtained by another method.^{17,32)} Even though a simple model of carrier propagation is proposed, the fundamental physical concept is correct and experimentally verified.

Additionally, we can discuss the relation with the MW model. Recently it was shown^{16,33)} that the interface charging can be used to model the pentacene–gate insulator interface below the source electrode. In the MW model, the concept of contact resistance has been treated by a relation for charge transport similar to eq. (14). However, the meaning is different; the MW model describes a steady state, and the idea is based on the presence of an interface charge caused by an electric field across the interface and a difference in relaxation times, whereas the TLA model explains charge propagation in the channel region and does not require contact resistance.

Note that a model for the pentacene film with distributed R and C elements [see Fig. 2(b)] instead of a simple resistance R can be used for the organic active layer in an OFET. However, in this case the relaxation times of all repeat unit (RC loops) are identical, thus no charge is accumulated in the pentacene film unlike in the case of the MIM device. Nevertheless, the charge is accumulated

at the pentacene–gate insulator interface and this interface charging is done together with the charge transport. Therefore, the proposed TLA model describes a more realistic situation in comparison with a standard steady state MW model where at first charge is accumulated according to the MW effect, caused by the relaxation time difference between adjacent active and gate insulator layers, and only subsequently it is transported. However, we must point out that also the MW model can be extended for the case of time-dependent fields with the same result as TLA. Curiously, the transit time through the OFET device is also the relaxation time of the investigated device. In other words, charging of the OFET represents a way how charge is transported in a three-electrode system. In contrast to the MIM structure here it is possible to store an electric charge in the device by the charging process of the interface. Therefore, this result stimulates us to extend TLA model and study charge propagation up to the channel end.

Interestingly, the drain–source current can be defined as a total charge accumulated in the channel region Q_s ($= \int_0^L q_s dx$), which is transported in time t_{tr} , i.e., $I_{ds} = Q_s/t_{tr}$. Therefore, the drain–source current can be obtained as

$$I_{ds} = \int_0^{V_{ds}} \frac{C_{ch}}{t_{tr}} dV = C_g \mu \frac{W}{L} \left(V_{gs} - V_{th} - \frac{1}{2} V_{ds} \right) V_{ds}, \quad (17)$$

where the charge is obtained by integration of the gate dielectric capacitance ($C_{ch} = C_g WL$) over the voltage across the channel (i.e., the potential difference between source and drain electrodes, the drain–source voltage).

The TLA theory predicts a reflection of the propagating signal in the case where the resistance at the end of the transporting channel is different from the characteristic impedance. Therefore, it is important to estimate the characteristic impedance of the OFET channel. The impedance is defined as a ratio of voltage V and current I ,

$$Z = \frac{V}{I}, \quad (18)$$

where V is the potential of the signal propagating through the channel [i.e., $V_{gs} - V_{th}$, see eq. (14)] and current I represents the charge flow,

$$I = \frac{dQ_s}{dt}. \quad (19)$$

The increment of the charge dQ illustrates a charging of the infinitesimally small capacitance dC by voltage V . The increase of the capacitance is related to the propagation, hence

$$dC = C' v dt, \quad (20)$$

where C' is the capacitance per unit of length ($C' = C_g W$) and v is the group velocity, which can be obtained by the differentiation of eq. (14),

$$v = \left(\frac{dt}{dL} \right)^{-1} = \frac{\mu \left(V_{gs} - V_{th} - \frac{1}{2} V_{ds} \right)}{L}. \quad (21)$$

Substituting above-mentioned relations into eq. (18) one obtains the characteristic impedance of the channel

$$Z_{ch} = \frac{1}{C'v}. \quad (22)$$

Curiously, the characteristic impedance of the channel is a function of the channel length ($Z_0 \propto L$), voltage [$Z_{ch} \propto 1/(V_{gs} - V_{th} - V_{ds}/2)$], and channel width ($Z_{ch} \propto 1/W$). Note that the characteristic impedance reaches two times higher value than the channel resistance, $Z_{ch} = 2R_{ch}$. In accordance to the comparison of the MW model [eq. (7)] and TLA [eq. (14)] we conclude that this factor of 2 has an origin in the time-dependent conductivity during the charge carriers propagation. Of course, in our investigated OFET system the terminal resistance is represented by the contact resistance of the drain electrode. Therefore, in the case of no impedance (resistance) matching, after application of the pulse voltage the backward-travelling wave from the edge of the pentacene film is expected. For typical values of the experimental variables ($L = 50 \mu\text{m}$, $\mu = 0.1 \text{ cm}^2 \text{ V}^{-1} \text{ s}^{-1}$, $V_{gs} - V_{th} - V_{ds}/2 = -10 \text{ V}$ and $C_g = 5.4 \text{ nF/cm}^2$) we obtain a characteristic impedance $Z_0 \sim 5 \text{ M}\Omega$. Obtained characteristic impedance corresponds to the optimal contact resistance of the drain electrode and the presence of a higher value is related to the potential drop on the electrode.

5. Conclusions

Although in the MIM structure (two-electrode system) the charge transport can be expressed as a drift of carriers driven by the voltage applied between electrodes, in the OFET structure (three-electrode system) charge transport is not only due to the source–drain bias but also due to an interface charge propagation, and thus, depends on the gate–source voltage. Two different model are carried out to discuss charge propagation on the organic semiconductor–gate insulator interface. The MW model explanation has deep physical insight to the charge accumulation phenomenon and the discussion based on TLA is more suitable for charge propagation in the channel region with variable electric field, which is visualized by the TRM-SHG technique. In other words, it can be explained as the charge accumulation and propagation, where charge transport is realized by the creation of the accumulated charge on the organic semiconductor–gate insulator interface. Additionally, the TLA approach with distributed parameters give us almost identical result also for case of variable electric field, which is uncommon for impedance spectroscopy analysis. Moreover, simple analysis showed that in the MIM structure all charge is transported, whereas in the OFET structure charge is accumulated on the interface in the meaning of the MW effect. Proposed theoretical results are extension of previous small-signal analysis elaborated for the impedance spectroscopy measurements and are in accordance with the TRM-SHG experiment with a voltage pulse applied to the source electrode or to the source and drain electrodes at once. Propagation of interface charging was also used for the evaluation of the characteristic impedance for the drain electrode and determination of the drain–source current. This discussion points out differences in the charge transport mechanism, which has an affect on the mobility evaluation from the transit time measurements.

Acknowledgement

One of the authors (M.W.) thanks support from Slovak Research and Development Agency (APVV, Grant No. LPP-0175-09).

- 1) H. E. Katz: *J. Mater. Chem.* **7** (1997) 369.
- 2) H. E. Katz: *Chem. Mater.* **16** (2004) 4748.
- 3) H. Sirringhaus: *Adv. Mater.* **17** (2005) 2411.
- 4) M. Mas-Torrent and C. Rovira: *Chem. Soc. Rev.* **37** (2008) 827.
- 5) L. Bürgi, T. J. Richards, R. H. Friend, and H. Sirringhaus: *J. Appl. Phys.* **94** (2003) 6129.
- 6) C. W. Tang and S. A. VanSlyke: *Appl. Phys. Lett.* **51** (1987) 913.
- 7) C. Kim, A. Facchetti, and T. J. Marks: *Science* **318** (2007) 76.
- 8) T. Minari, T. Nemoto, and S. Isoda: *J. Appl. Phys.* **99** (2006) 034506.
- 9) D. Knipp, R. A. Street, and A. Völkel: *J. Appl. Phys.* **93** (2003) 347.
- 10) E. Pavlica and G. Bratina: *J. Phys. D* **41** (2008) 135109.
- 11) L. Dunn, D. Basu, L. Wang, and A. Dodabalapur: *Appl. Phys. Lett.* **88** (2006) 063507.
- 12) D. Basu, L. Wang, L. Dunn, B. Yoo, S. Nadkarni, A. Dodabalapur, M. Heeney, and I. McCulloch: *Appl. Phys. Lett.* **89** (2006) 242104.
- 13) R. Dost, A. Das, and M. Grell: *J. Appl. Phys.* **104** (2008) 084519.
- 14) K. D. Jung, C. A. Lee, D. W. Park, B. G. Park, H. Shin, and J. D. Lee: *IEEE Electron Device Lett.* **28** (2007) 204.
- 15) D. M. Taylor, D. L. John, and J. A. Drysdale: *Mater. Res. Soc. Symp. Proc.* **1003E** (2007) 1003-O05-07.
- 16) J. Lin, M. Weis, T. Manaka, and M. Iwamoto: *Thin Solid Films* **518** (2009) 448.
- 17) T. Manaka, F. Liu, M. Weis, and M. Iwamoto: *Phys. Rev. B* **78** (2008) 121302(R).
- 18) T. Manaka, E. Lim, R. Tamura, and M. Iwamoto: *Nat. Photonics* **1** (2007) 581.
- 19) L. Bürgi, R. H. Friend, and H. Sirringhaus: *Appl. Phys. Lett.* **82** (2003) 1482.
- 20) J. C. Maxwell: *A Treatise on Electricity and Magnetism* (Dover, New York, 1954) 3rd ed., Vol. 1, Chap. X, p. 450.
- 21) K. W. Wagner: *Arch. Elektrotech.* **2** (1914) 371 [in German].
- 22) M. A. Lampert and P. Mark: *Current Injection in Solids* (Academic, New York, 1970).
- 23) P. Parisse, M. Passacantando, S. Picozzi, and L. Ottaviano: *Org. Electron.* **7** (2006) 403.
- 24) R. Tamura, E. Lim, T. Manaka, and M. Iwamoto: *J. Appl. Phys.* **100** (2006) 114515.
- 25) R. G. Kepler: *Phys. Rev.* **119** (1960) 1226.
- 26) W. E. Spear and J. Mort: *Proc. Phys. Soc.* **81** (1963) 130.
- 27) H. Scher and W. Montroll: *Phys. Rev. B* **12** (1975) 2455.
- 28) N. Karl: *Synth. Met.* **133** (2003) 649.
- 29) M. Weis, T. Manaka, and M. Iwamoto: *J. Appl. Phys.* **105** (2009) 024505.
- 30) G. Horowitz: in *Organic Electronics*, ed. H. Klauk (Wiley-WCH, Weinheim, 2006) p. 10.
- 31) T. Manaka, Y. Suzue, and M. Iwamoto: *Jpn. J. Appl. Phys.* **44** (2005) 2818.
- 32) M. Weis, J. Lin, D. Taguchi, T. Manaka, and M. Iwamoto: *J. Phys. Chem. C* **113** (2009) 18459.
- 33) E. Lim, T. Manaka, and M. Iwamoto: *J. Appl. Phys.* **104** (2008) 054511.